Available online at www.sciencedirect.com
ScienceDirect
Journal of Hazardous Materials 156 (2008) 604–611
Journal of Hazardous Materials
www.elsevier.com/locate/jhazmat

An approach for evaluating nanomaterials for use as packed bed adsorber media: A case study of arsenate removal by titanate nanofibers

Kiril Hristovski [a,*], Paul Westerhoff [b,1], John Crittenden [b,2]

[a] *Environmental Technology Laboratory, Arizona State University – Polytechnic Campus, 6075 S. WMS Campus Loop W, Mesa, AZ 85212, USA*
[b] *Department of Civil and Environmental Engineering, Arizona State University, Box 5306, Tempe, AZ 85287-5306, USA*

Received 16 October 2007; received in revised form 17 December 2007; accepted 18 December 2007
Available online 26 December 2007

Abstract

The primary goal of this paper is to propose a series of logical testing steps to determine whether a new adsorbent media is suitable for application in packed bed configurations for treating drinking water pollutants. Although the focus of the study is placed on titanate nanofibers, as a never before tested media for arsenate removal, the set of testing processes that encompasses nanomaterial characterization, equilibrium and kinetics tests, and modeling, can be used on any material to quickly determine whether these materials are suitable for water treatment applications in a packed bed configurations. Bundle-like titanate nanofibers were produced by an alkaline synthesis method with Degussa P25 TiO_2. The synthesized nanofibers have a rectangular ribbon-like shape and exhibited large surface area (126 $m^2\,g^{-1}$) and high adsorbent porosity ($\varepsilon_P \approx 0.51$). Equilibrium batch experiments conducted in 10 mM $NaHCO_3$ buffered ultrapure water at three pH values (6.6, 7.6 and 8.3) with 125 $\mu g\,L^{-1}$ As(V) were fit with the Freundlich isotherm equation ($q = K \times C_E^{1/n}$). The Freundlich adsorption intensity parameter ($1/n$) ranged from 0.51 to 0.66, while the capacity parameters (K) ranged from 5 to 26 $\mu g\,g^{-1}$. The pore diffusion coefficient and tortuosity were estimated to be $D_P \approx 1.04 \times 10^{-6}\,cm^2\,s^{-1}$, and $\tau \approx 4.4$. For a packed bed adsorbent operated at a realistic loading rate of 11.6 $m^3\,m^{-2}\,h^{-1}$ with particles obtained by sieving the media through US mesh 80 × 120, the external mass transport coefficient was estimated to be $k_f \approx 8.84 \times 10^{-3}\,cm\,s^{-1}$. In this study, surface diffusion was ignored because the adsorbent has high porosity. Pore surface diffusion model (PSDM) was used to predict the arsenate breakthrough curve, and a short bed adsorbent (SBA) test was conducted under the same conditions to verify validity of the estimated values. There was no titanium release in the treated effluent during the SBA test. The pore Biot number ($Bi_P > 100$) implied that pore intraparticle resistance controls the overall mass transport. The PSDM was used to predict arsenate breakthrough in a simulated full-scale system. The overall combined use of modeling, material characterization, equilibrium, and kinetics tests was easier, cheaper and faster than a long duration pilot tests. While the conclusion regarding the titanate nanofibers is that they are less suitable for arsenate removal from water than commercially available media, there may be other applications where this novel nanomaterial may be suitable because of unique surface chemistry and porosity.

Keywords: Arsenate; Titanium; Nanofibers; Water; Packed bed

1. Introduction

The unique characteristics of nanomaterials such as large surface area and specific functionality have lead to numerous reports of their potential use as adsorbents to remove pollutants from water. Two common approaches for using adsorbents in full-scale application are either suspended adsorbent or packed bed reactors. Unfortunately, it may be extremely difficult to remove essentially 100% of the nanomaterials in suspended adsorbent reactors, even if the nanomaterials have unique properties (e.g. magnetic) [1]. It is far more likely that packed bed reactors with some form of aggregated nanomaterial adsorbent media may be utilized to prevent release of nanomaterials into finished water. Aggregated nanomaterials may become diffusion limited, and as such addressing this issue is critical in assessing the viability of nanomaterial adsorbents in full-scale systems.

In the past decade, Kasuga et al. [2], Yuan and Su [3], and Peng et al. [4] report fabricating bundle-like titanate nanofibers with high surface area. Since it has been reported in the literature that titania-based adsorbents can remove arsenic, it is reasonable

* Corresponding author. Tel.: +1 480 727 1132; fax: +1 480 727 1684.
E-mail addresses: kiril.hristovski@asu.edu (K. Hristovski), p.westerhoff@asu.edu (P. Westerhoff), jcritt@asu.edu (J. Crittenden).
[1] Tel.: +1 480 965 2885; fax: +1 480 965 0557.
[2] Tel.: +1 480 965 3420; fax: +1 480 965 0557.

0304-3894/$ – see front matter © 2007 Elsevier B.V. All rights reserved.
doi:10.1016/j.jhazmat.2007.12.073

to postulate that bundle-like titanate nanofibers can potentially be used as nanostructured adsorbents [5–8]. Therefore, one focus of the study is to explore whether these bundle-like nanofiber structures can be used as adsorbent for arsenic treatment using continuous-flow water treatment applications. Arsenate was selected as a target contaminant because of its potential health and regulatory concerns as well as its ability to adsorb onto metal (hydr)oxide surfaces by forming inner-sphere bidentate ligands [9,10]. Arsenic is classified as a Class A human carcinogen by the International Agency for Research on Cancer and is an emerging contaminant in water in many regions of the world [11,12].

While one focus of this study is to evaluate the suitability of the titanate nanofibers as adsorbent media in a continuous flow packed bed reactor for removing arsenate from water, the main goal is to propose and evaluate series of steps that should be followed when developing new adsorbent media for application in packed bed configurations for treating drinking water pollutants. The use of titanate nanofibers for arsenate removal serves as a case study of this process. The following steps were undertaken to evaluate titanate nanofibers for arsenic removal while demonstrating a logical testing protocol for new nanomaterial water treatment systems: (1) fabricate titanate nanofibers using an existing method; (2) characterize nanofibers by powder X-ray diffraction (XRD), energy dispersive X-ray microanalysis (EDX), focused ion beam/scanning electron microscopy (FIB/SEM) techniques, and surface charge and surface area analysis; (3) conduct adsorption isotherm tests and dynamic packed bed column tests for arsenate removal in bicarbonate buffered ultrapure water; (4) evaluate loss of adsorbent from the packed bed column; (5) quantify mass transport processes that control the rate of arsenate adsorption in a packed bed column; (6) predict the performance of full-scale systems using the pore surface diffusion model (PSDM).

2. Experimental approach

2.1. Preparation of titanate nanofibers

Bundle-like titanate nanofibers were fabricated using the alkaline synthesis method developed and studied by Kasuga et al. [2] Yong and Su [3], and Peng et al. [4]. Briefly, 10 g of Aeroxide P25 TiO_2 nanopowder (Degussa, Germany), as a precursor material, was suspended in 100 mL of 10 M NaOH and sealed in a 125 mL Teflon vessel. The vessel was heated for a period of 48 h at $125 \pm 5\,^{\circ}C$. After the vessel was cooled, the treated material was repeatedly washed with ultrapure water ($<1\,\mu S\,cm^{-1}$) and 1% nitric acid solution and centrifuged at $F > 1300$ G until the pH of the suspension was ≤ 7 and the excess TiO_2 particles were removed. The thick suspension was air-dried at $T = 20 \pm 2\,^{\circ}C$ in a negative pressure environment until dry and hard cake was formed. The cake was then crushed and sieved to 80×120 mesh size using US standard mesh sieves, and the particle size was estimated using scanning electron microscopy technique (SEM XL 30 by FEI). The size of the crushed media particles generally ranged from 150 to 400 μm (Fig. 1a), so geometric mean of ~250 μm was considered for purposes of the study.

2.2. Media characterization

Material analysis employed EDX microanalysis (EDAX Inc.) for the chemical composition, FIB/SEM for the size and the shape (Nova 200 NanoLab UHR FEG-SEM/FIB), and XRD for the chemical structure (Bruker SMART APEX). Zeta potential (ζ) was measured using a phase analysis light scattering technique (ZetaPALS, Brookhaven Instrument Corporation) in a 10 mM KNO_3 background electrolyte solution; pH was adjusted using KOH and/or HNO_3. Surface area was measured using N_2 adsorption approach (multipoint point BET method, Micromeritics ASAP 2020). Adsorbent media density and porosity were evaluated following a procedure described in Sontheimer et al. [13]. Assuming cylindrical pores, the average pore diameter was calculated from the surface area–pore volume ratio as suggested by Crittenden et al. [14]:

$$\frac{2}{r_{pore}} = \frac{A_{ad}}{V_{ad}} \tag{1}$$

where r_{pore} is the average pore radius (m); A_{ad} is the surface area of the adsorbent (m^2); and V_{ad} is the pore volume of the adsorbent (m^3).

2.3. Equilibrium adsorption experiments

Batch arsenate adsorption experiments with nanofibers were conducted at three pH values of 6.6 ± 0.1, 7.6 ± 0.1, and 8.3 ± 0.1 (final pH values) in 10 mM $NaHCO_3$ buffered ultrapure water and initial arsenate concentration $C_0 \approx 125\,\mu g\,L^{-1}$. Adsorption experiments with the initial P25 TiO_2 were only conducted at pH 7.6 ± 0.1. All experiments were conducted in 50 mL centrifuge vials with adsorbent dosages of $17\,mg\,L^{-1}$ to $2.8\,g\,L^{-1}$. Although complete adsorption of arsenate onto titanium (hydr)oxide surfaces occurs within few hours, samples were continuously agitated for 3 days prior to ensure complete pseudo equilibrium [6]. Centrifugation ($F > 1300$ G) was used to remove the adsorbent from the suspension. Adsorption isotherms were developed and analyzed using the Freundlich adsorption isotherm model (Eq. (1)).

$$q = K \times C_E^{1/n} \tag{2}$$

where q is adsorption capacity, K is the Freundlich adsorption capacity parameter, C_E is the equilibrium concentration of adsorbate in solution, and $1/n$ is the Freundlich adsorption intensity parameter.

2.4. Continuous flow column tests and adsorption modeling

Initial estimates for the external mass transport coefficient were based on the Gnielinski correlation [13]:

$$k_f = \frac{[1 + 1.5(1-\varepsilon)] \times D_l}{d_p} \times (2 + 0.644 \times Re^{1/2} \times Sc^{1/3}) \tag{3}$$

$$Re = \frac{\rho_l \times \Phi \times d_p \times v_l}{\varepsilon \times \mu_l} \tag{4}$$

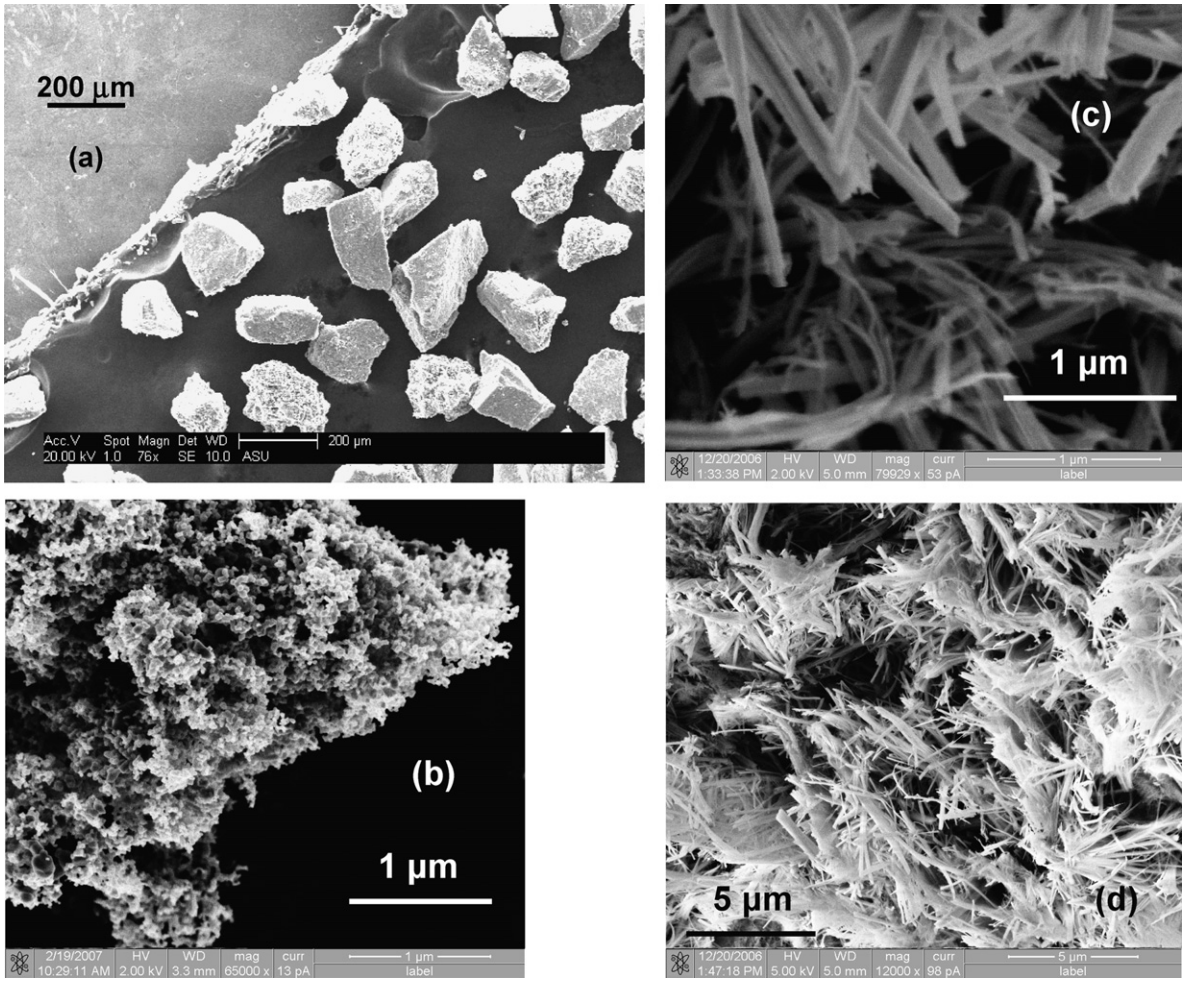

Fig. 1. SEM of (a) titanate nanofiber media particles used in the short bed adsorber tests and FIB/SEM of (b) Aeroxide P25 TiO_2, (c and d) titanate nanofibers.

$$Sc = \frac{\mu_l}{\rho_l \times D_l} \tag{5}$$

constrains: $Re \times Sc > 500$; $0.6 \leq Sc \leq 10^4$; $1 \leq Re < 100$; $0.26 < \varepsilon < 0.935 k_f$ is the external mass transport coefficient (calculated $k_f \approx 8.84 \times 10^{-3}\,\mathrm{cm\,s^{-1}}$); Re is the Reynolds number (unitless); Sc is the Schmidt number (unitless); d_p is the adsorbent particle diameter ($d_p = 0.250 \times 10^{-3}$ m); D_l is the free liquid diffusivity for arsenate ($D_l = 9.05 \times 10^{-10}\,\mathrm{m^2\,s^{-1}}$) [15]; ε is the bed void fraction ($\varepsilon \approx 0.387$); μ_l is the dynamic viscosity of water at 20 °C ($1.002 \times 10^{-3}\,\mathrm{N\,s\,m^{-2}}$); ρ_l is the density of water at 20 °C ($\rho_l = 998.2\,\mathrm{kg\,m^{-3}}$); Φ is the particle shape factor ($\Phi = 1.2$); v_l is the liquid superficial velocity ($v_l \approx 0.00318\,\mathrm{m\,s^{-1}}$).

Considering that the material was very porous (the particle porosity $\varepsilon_P \approx 0.507$), pore diffusion was the assumed dominant intraparticle mass transport over the surface diffusion, and the impact of surface diffusion was assumed negligible. As suggested by Sontheimer et al. [13], the pore diffusion coefficient was estimated using Eq. (6):

$$D_P = \frac{\varepsilon_P \times D_l}{\tau} \tag{6}$$

The tortuosity of was estimated using the correlation suggested by Mackie and Meares (Eq. (7)) for electrolyte solutions [16]:

$$\tau = \frac{(2 - \varepsilon_P)^2}{\varepsilon_P} \tag{7}$$

where τ is the toruosity factor; and ε_P is the particle porosity ($\varepsilon_P \approx 0.507$). The estimated toruosity value was $\tau \approx 4.4$, which does not seem unreasonable considering the estimated average pore size was $d_{Pore} \approx 18$ nm, and the diameter of the arsenate ion, $d_{As} \approx 0.8$ nm [17]. This value fits within the expected range for tortuosities of porous solids ($2 \leq \tau \leq 6$) such as silica gel or alumina [18]. The estimated value for the pore diffusion coefficient was $D_P \approx 1.04 \times 10^{-6}\,\mathrm{cm^2\,s^{-1}}$.

The pore and surface diffusion model was used to provide initial predictions of the arsenate breakthrough curve, and to validate the assumption that surface diffusion can be ignored [19–21]. PSDM is a dynamic packed bed model that incorporates a set of assumptions and governing partial differential equations describing the adsorber dynamics in a packed bed setup. PSDM simulations were conducted using AdDesignS^{TM} software (Michigan Technological University) [22].

To validate the calculated k_f and D_P values, and to confirm negligible effect of D_S on the overall mass transport, a short bed adsorber (SBA) test was conducted. SBA tests are continuous flow column experiments with a packed bed sufficiently long enough to describe dissolved pollutant mass transfer zone [23,24]. The initial model estimates predicted that a SBA column with diameter of 1.1 cm and bed depth of 1.4 cm with adsorbent particle of 0.0250 cm should be sufficiently long enough to describe dissolved pollutant mass transfer zone at loading rate of 11. 6 $m^3\,m^{-2}\,h^{-1}$, initial arsenate concentration C_0 of 122 $\mu g\,L^{-1}$ and temperature of 20 °C. Such loading rates are typical for full-scale packed bed column absorbers [7,25,26].

For the SBA test, a 1.4 cm deep adsorbent media bed was packed atop a support of quartz sand and metal support screen in a glass column with diameter (d_{Column}) of 1.1 cm (Ace Glass). Glass beads were placed above and below to provide evenly distributed flow. Adsorbent media sieved through US mesh size 80 × 120 was used to provide d_{Column}/d_p ratio of ~44. According to Benenati and Brosilow [27] and Chu and Ng [28], the wall effect on the mass transfer can be neglected for d_{Column}/d_p ratios >20. Since minimum of 30 mL of sample volume was needed to conduct the necessary analyses, effluent from the SBA test was collected in ~20 bed volume (BV) sample aliquots.

The relative importance of internal and external mass transport resistance was evaluated by estimating the pore (Bi_P) Biot numbers using the relationship given by [13]:

$$Bi_P = \frac{k_f \times d_P}{2 \times D_P} \quad (8)$$

where d_P is the geometric mean of the media (cm).

The PSDM was used to model the performance of full-scale fix bed systems operating at 12 $m^3\,m^{-2}\,h^{-1}$, and different empty bed contact times (EBCTs) (20, 40, and 80 min). To maintain the same loading rate, the length of the packed bed was changed to achieve the desired EBCTs. The modeling was conducted with realistic values of $C_0 = 25\ \mu g\,L^{-1}$. Since the external mass transport is a function of the loading rate and the particle size, k_f was recalculated for $d_p = 0.8$ mm and $\Phi = 1.2$ using Eq. (3). The water chemistry, pH, and bed porosity were assumed the same as ones used in the SBA test.

2.5. Titanium and arsenic analysis

The loss of the adsorbent from the packed bed column was evaluated by digesting 20 mL aliquots of column effluent in concentrated HNO_3/H_2SO_4 (Standard Methods 3030 D and 3030 G) and analyzing the titanium concentration using a graphite furnace atomic absorption spectrophotometer (GF-AAS) Varian Zeeman Spectra 400 with GTA 96 system [29].

Arsenate was analyzed using a graphite furnace atomic absorption spectrophotometer (GF-AAS) Varian Zeeman Spectra 400 with GTA 96 system.

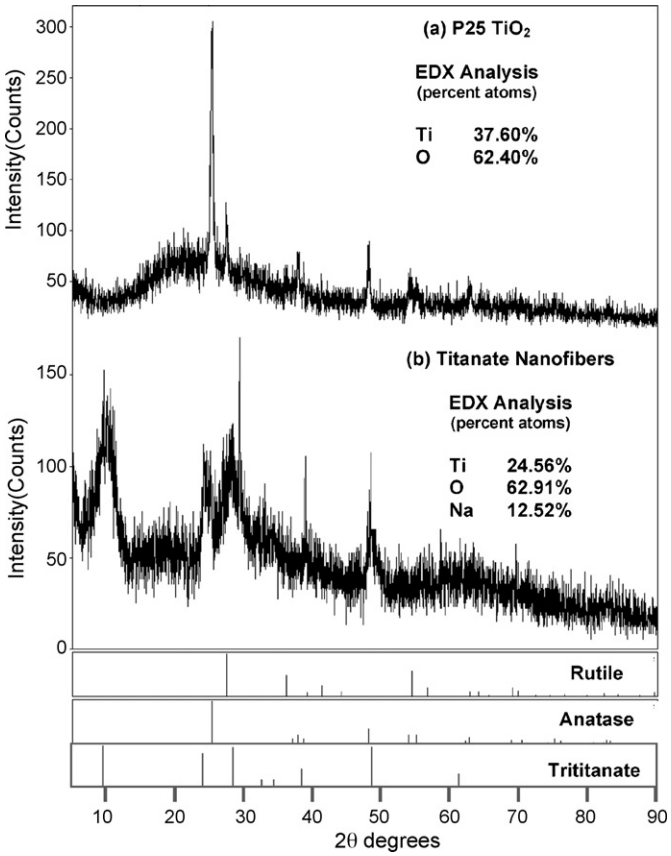

Fig. 2. X-Ray diffraction spectra and EDX microanalysis for (a) Aeroxide P25 TiO_2 and (b) titanate nanofibers.

3. Results and discussion

3.1. Media characterization

The P25 TiO_2 precursor material used to fabricate the nanofibers consists of nanoparticles with sizes $d_P \leq 100$ nm, which are aggregated together into micron size aggregates (Fig. 1b). This observation is consistent with other reports [30–32]. EDX analysis confirmed that the TiO_2 precursor mate-

Table 1
Properties and Freundlich isotherm adsorption parameters of Aeroxide P25 TiO_2 and titanate nanofibers

Material	Surface area ($m^2\,g^{-1}$)	pH_{IEP}	pH	Zeta potential ζ (mV)	K^a	K^b	$1/n$ (unitless)
P25 TiO_2	53	5.7	7.6 ± 0.1	−24	2.71	143	0.38
Titanate nanofibers	126	3.0	6.6 ± 0.1	−25	0.17	26	0.66
			7.6 ± 0.1	−28	0.17	22	0.51
			8.3 ± 0.1	−34	0.04	5.0	0.57

[a] $(\mu g\,m^{-2})(L\,\mu g^{-1})^{1/n}$.
[b] $(\mu g\,g^{-1})(L\,\mu g^{-1})^{1/n}$.

rial consists of both anatase and rutile (Fig. 2a). Table 1 summarizes the properties of P25 TiO_2 precursor material.

Fig. 1c and d illustrates that the fabricated adsorbent media consists of bundle-like titanate nanofibers of ribbon-like or rectangular in shape ~4 μm long and 30–100 nm thick. The surface area was 126 $m^2\,g^{-1}$, which is almost 2.5 times greater than one of the P25 TiO_2 precursor material (53 $m^2\,g^{-1}$). EDX of the nanofibers indicated a different elemental composition from P25 TiO_2 precursor material (Fig. 2b). According to Yuan and Su [3], Chen et al. [33], and Chen et al. [34], diffraction peaks with 2θ angles at ~10–12°, ~25–30° and ~50° are indication of trititanate. The broadening of the diffraction peaks is due to the nanometer size of the fibers and bending of some atom planes of the fibers. The high scattering exhibited in the XRD spectrum for the nanofibers suggest non-crystalline structure. Although the XRD 2θ values for the nanofibers' diffraction peaks in Fig. 2b suggest a structure that can be indexed as trititanate, EDX indicates a ratio of the percent atoms Na:Ti:O ≈ 12.5:25:63. Thus, nanofibers may be monosodium titanate ($NaTi_2O_5$) or sodium hydrogen dititanate ($NaHTi_2O_5$), considering that EDX cannot detect hydrogen atoms.

The material density of the nanofibers was $\rho_M \approx 1.77\,g\,cm^{-3}$, and the particle density was $\rho_P \approx 0.876\,g\,cm^{-3}$. The porosity of the titanate nanofiber particles was $\varepsilon_P \approx 0.507$. From Eq. (1), the average pore diameter was estimated to be $d_{pore} \approx 18$ nm indicating that the titanate nanofiber particles are microporous according to the IUPAC classification [14].

The *iso*-electric points (pH_{IEP}) and zeta potential at specific pH values of the titanate nanofibers and P25 TiO_2 are given in Table 1. Measured zeta potentials were similar in the pH range between 6.6 and 8.3. The pH_{IEP} of P25 TiO_2 was almost 2.7 pH units higher than the pH_{IEP} of the nanofibers. However, the zeta potential of the nanofibers at pH 7.6 was only 4 mV lower the zeta potential of the P25 TiO_2 at pH 7.6 (Table 1).

3.2. Equilibrium adsorption experiments

Fig. 3 presents the arsenate adsorption isotherms with adsorption density normalized per surface area of adsorbent (P25 TiO_2 or nanofibers). Table 1 summarizes Freundlich isotherm adsorption parameters for the equilibrium experimental conditions. Arsenate adsorption is highest at pH 6.6 ± 0.1, and lowest at pH 8.3 ± 0.1 for the titanate nanofibers. Since arsenate is characterized with $pK_{a2\text{-Arsenate}} = 6.8$ and $pK_{a3\text{-Arsenate}} = 11.6$, $H_2AsO_4^-$ and $HAsO_4^{2-}$ species will be dominant in waters with pH between 6 and 9 typically found in the environment [5,12]. At higher pH, $HAsO_4^{2-}$ is more dominant specie than $H_2AsO_4^-$ and, as such, it will tend to adsorb less onto a negatively charged surface.

Despite the higher surface area of the nanofibers, the titanate nanofibers have a lower arsenate adsorption capacity than P25 TiO_2 at pH 7.6 (Fig. 3 and Table 1). The Freundlich adsorption intensity parameters were $0.51 \le 1/n \le 0.66$ for the nanofibers, and $1/n = 0.38$ for P25 TiO_2, suggesting favorable adsorption processes (i.e. $1/n < 1$) for both media.

3.3. SBA test and PSDM modeling

Fig. 4 presents the predicted arsenate breakthrough curve SBA tests conducted at loading rate of 195 $L\,m^{-2}\,min^{-1}$ (~4.8 $gal\,min^{-1}\,ft^{-2}$; $Re \times Sc \approx 2830$) and initial arsenate concentration $C_{0(As)} \approx 122\,\mu g\,L^{-1}$. As illustrated, breakthrough occurred rapidly. Titanium concentrations in the sample aliquots were below the instrument's detection limit for titanium ($MDL_{Ti} \sim 10\,\mu g\,L^{-1}$) indicating that the packed bed was stable and there was no adsorbent loss in the effluent.

For the initially estimated $k_f \approx 8.84 \times 10^{-3}\,cm\,s^{-1}$ and $D_P \approx 1.04 \times 10^{-6}\,cm^2\,s^{-1}$, the PSDM provided a good prediction (line in Fig. 4a) of the arsenate breakthrough. The predicted arsenate breakthrough curve did not change shape for

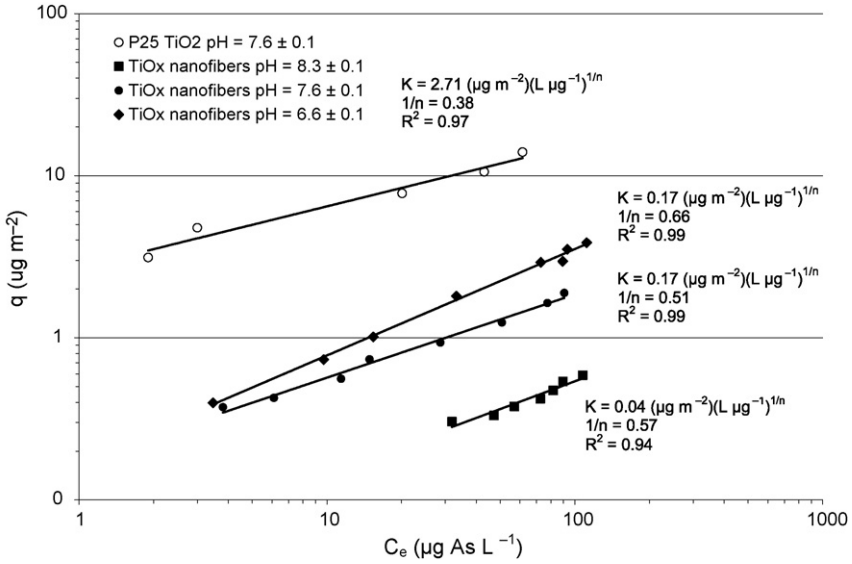

Fig. 3. Arsenate adsorption isotherms for Aeroxide P25 TiO_2 and titanate nanofibers in 10 mM $NaHCO_3$ buffered ultrapure water and contact time of 3 days. ($C_{0\text{-As(V)}} \approx 125\,\mu g\,L^{-1}$).

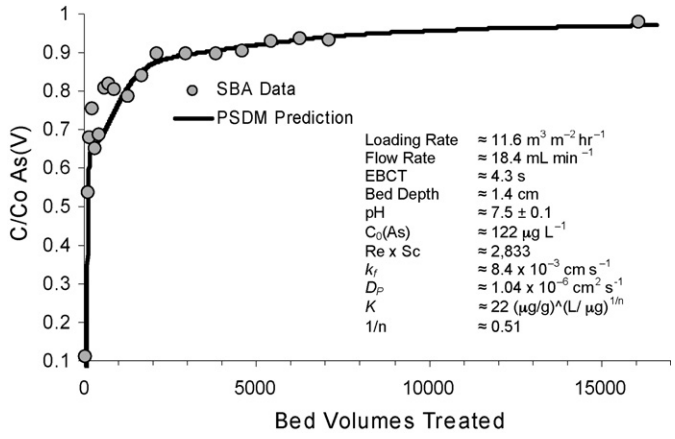

Fig. 4. Arsenate breakthrough curve for titanate nanofibers initial PSDM prediction and experimental data.

$D_S < 1 \times 10^{-10}$ cm^2 s^{-1} and provided the best fit with the experimental data. In contrast, $D_S \geq 1 \times 10^{-10}$ cm^2 s^{-1} predicted curves with shapes that were not consistent with the observed experimental data. Similar values for $D_S < 10^{-10}$ cm^2 s^{-1} have been reported for other media where arsenate adsorption occurs via inner-sphere complexation [25,35]. Experimental data verified that surface diffusion can be ignored considering that D_S is at least four orders of magnitude smaller than D_P.

The estimated Biot number (Bi_P) was >100 and implied that the pore diffusion controls the overall mass transport. A Biot number ≥20 implies intraparticle diffusion controls the overall mass transport of the system [13].

3.4. Performance of full-scale packed bed systems

As illustrated in Fig. 5, all modeled curves are characterized with initial rapid breakthrough for arsenate. This rapid breakthrough is expected as the adsorption sites located on the outermost surfaces of the particle become quickly occupied with arsenate due to the low adsorption capacity, and the only available sites are deeper inside the particle. The gradual breakthrough following the rapid increase is also expected later in the run as the intraparticle mass transport becomes more limiting due to diffusion of arsenate ions deeper inside the pores of the particle to find available adsorption sites. To improve the overall system kinetics, the pore diffusion can be facilitated by shortening the path that arsenate ions travel inside the particle, which can be achieved by engineering a system with smaller adsorbent particles. This will also result in increase of the external mass transfer rate, which is particle size dependant. However, there are a few drawbacks that can result from using adsorbent media with small particle size. Increase in head loss, channeling, and loss of adsorbent have to be also considered when engineering adsorbent systems with small media particles.

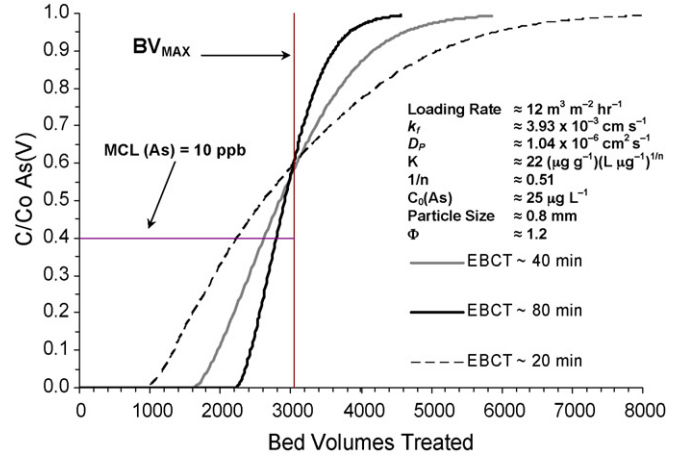

Fig. 5. Arsenate breakthrough curve for titanate nanofibers PSDM predictions for a full-scale system at EBCT = 20, 40, and 80 min.

Another way to obtain improved overall performance of the system (i.e. to treat greater number of bed volumes) is to properly engineer the packed bed. As illustrated in Fig. 5, the PSDM predicted that only ~2250 bed volumes can be treated at EBCT of 20 min before effluent concentration reached the maximum contaminant level (MCL) of 10 µg L^{-1} ($C/C_0 = 0.4$). However, the number of treated bed volumes before reaching the MCL increased to ~2600 and ~2800 with increase of the EBCT to 40 and 80 min, respectively, implying that more bed volumes can be treated by extending the EBCT. The maximum number of bed volumes treated (BV_{MAX}) can be estimated using the relationship suggested by Sontheimer et al. [13]:

$$BV_{MAX} = \frac{q_0 \times \rho_{BED}}{C_0} \times 1000 \quad (9)$$

where ρ_{BED} is the bed density of the packed bed ($\rho_{BED} \approx 0.68$ g cm^{-3}); q_0 is the adsorption capacity calculated at C_0. The multiplication factor results from the unit conversion. The maximum number of bed volumes that could be treated was estimated to approximately 3100 as illustrated in Fig. 5.

3.5. Comparison of the titanate nanofibers with commercially available media for arsenate treatment

Under same water chemistry and pH conditions, commercially available aggregated titanium dioxide nanoparticle medias (MetsorbG and Adsorbsia GTO) exhibited more than 40 times greater equilibrium adsorption capacity than the nanofibers [7]. However, the smaller average pore diameter of Adsorbsia GTO (9.4 nm), can contribute to increase in tortuosity and reduction of the pore diffusion rate resulting in slower kinetics than the titanate nanofibers [36]. Materials such as granulated ferric hydroxide (GFH) or activated alumina are cheaper to use because of their low cost and higher adsorption capacities than the titanate nanofibers, but their slower intraparticle mass transport could significantly impact the overall performance of the media in a packed bed column setup [16,25,35,36].

From a broader perspective, the durable titanate nanofibers may be well suited to remove different pollutants from water or other applications where titanate minerals have unique properties. There are studies reporting that titanates may be suitable for removal of heavy metals of the actinide series from nuclear waste solutions [37,38]. Other reports state that titanate-based media can be used to remove bivalent cations such as copper, nickel, cadmium, and zinc from aqueous solutions [39,40].

Beyond arsenate, a large number of contaminants pose health or environmental problems for which titanate nanomaterial-based media could be considered.

4. Conclusions

This study demonstrated that titanate nanofibers can be synthesized into highly porous adsorbent media that removes arsenic from water in a continuous flow application without release of titania from the packed bed. For the case of titanate nanofibers, they do not seem as viable a technology for arsenic removal as other commercially available sorbents. However, the six-step process for evaluating this nanomaterial should be transferable to other nanomaterials as they are developed for contaminant removal applications. The full-scale packed bed simulation was significantly easier than producing hundreds of kilograms, which would have been necessary for a long-duration pilot test. The approach used in the case study focused on important aspects that have to be considered during development and design of nanomaterial-based treatment systems involving packed bed adsorption columns. Besides high adsorption capacity, development and design of such systems should consider pore diffusion, adsorbent particle size, and packed bed design as key factors that can improve the overall performance of a packed bed adsorbent.

Acknowledgements

Thanks to Hanhpuc Nguyen, Yang Zhang, Grant Baumgardner, Dewey Wong, Hal Berkowitz, Xiaotong Wei, Dr. Yongsheng Chen, Dr. Larry Olson, Dr. Ke Li, Dr. Jerry Lin, Dr. Thomas Groy, Dr. Thomas Schildgen, and the Center for Solid State Systems at Arizona State University. Funding for this research was provided by the USEPA grant # RD831713, and the Department of Technology Management, at Arizona State University.

References

[1] V. Colvin, Using magnetic nanoparticles in water treatment, Abstr. Pap. Am. Chem. Soc. 231 (March 26) (2006), 207- IEC.
[2] T. Kasuga, M. Hiramatsu, A. Hoson, T. Sekino, K. Niihara, Titania nanotubes prepared by chemical processing, Adv. Mater. 11 (1999) 1307–1311.
[3] Z.Y. Yuan, B.L. Su, Titanium oxide nanotubes, nanofibers and nanowires, Colloid. Surf. A 241 (1–3) (2004) 173–183.
[4] H. Peng, G. Li, Z. Zhang, Synthesis of bundle-like structure of titania nanotubes, Mater. Lett. 59 (2005) 1142–1145.
[5] P.K. Dutta, A.K. Ray, V.K. Sharma, F.J. Millero, Adsorption of arsenate and arsenite on titanium dioxide suspensions, J. Colloid Interface Sci. 278 (2) (2004) 270–275.
[6] M.E. Pena, G.P. Korfiatis, M. Patel, L. Lippincott, X.G. Meng, Adsorption of As(V) and As(III) by nanocrystalline titanium dioxide, Water Res. 39 (11) (2005) 2327–2337.
[7] K. Hristovski, A. Baumgardner, P. Westerhoff, Selecting metal oxide nanomaterials for arsenic removal in fixed bed columns: from nanopowders to aggregated nanoparticle media, J. Hazard. Mater. 147 (2007) 265–274.
[8] D. Mohan, C.U. Pittman, Arsenic removal from water/wastewater using adsorbents – a critical review, J. Hazard. Mater. 142 (2007) 1–53.
[9] D.M. Sherman, S.R. Randall, Surface complexation of arsenic(V) to iron(III) (hydr)oxides: structural mechanism from ab initio molecular geometries and EXAFS spectroscopy, Geochim. Cosmochim. Acta 67 (22) (2003) 4223–4230.
[10] G. Ona-Nguema, G. Morin, F. Juillot, G. Calas, G.E. Brown, EXAFS analysis of arsenite adsorption onto two-line ferrihydrite, hematite, goethite, and lepidocrocite, Environ. Sci. Technol. 39 (23) (2005) 9147–9155.
[11] US Department of Health and Human Services (Ed.), Toxicological profile for arsenic, US Department of Health and Human Services, Washington, DC, 2000.
[12] P.L. Smedley, D.G. Kinniburgh, A review of the source, behaviour and distribution of arsenic in natural waters, Appl. Geochem. 17 (5) (2002) 517–568.
[13] H. Sontheimer, J. Crittenden, S. Summers, Activated Carbon for Water Treatment, second ed., DVGW-Forschungsstelle, Engler-Bunte Institut, Universitat Karlsruhe, Karlsruhe, Germany, 1988.
[14] J.C. Crittenden, R.R. Trussell, D.W. Hand, K.J. Howe, G. Tchobanoglous (Eds.), Water Treatment: Principles and Design, second ed., Wiley & Sons, Inc., Hoboken, New Jersey, USA, 2005.
[15] D. Lide (Ed.), CRC Handbook of Chemistry and Physics, 87th ed., Talor and Francis Group, Boca Raton, Florida, 2006.
[16] D.M. LeVan, G. Carta, C.M. Yon, Adsorption and ion exchange, in: R.D. Perry, D.W. Green (Eds.), Perry's Chemical Engineers' Handbook, seventh ed., McGraw-Hill, New York, USA, 1997 (Chapter 16).
[17] T.F. Lin, J.K. Wu, Adsorption of arsenite and arsenate within activated alumina grains: equilibrium and kinetics, Water Res. 35 (8) (2001) 2049–2057.
[18] J.G. Knudsen, H.C. Hottel, A.F. Sarofim, P.C. Wankat, K.S. Knaebel, Heat and mass transfer, in: R.D. Perry, D.W. Green (Eds.), Perry's Chemical Engineers' Handbook, seventh ed., McGraw-Hill, New York, USA, 1997 (Chapter 5).
[19] G. Friedman, Mathematical modeling of multicomponent adsorption in batch and fixed-bed reactors, in: Master's Thesis, Michigan Technological University, Houghton, Michigan, 1984.
[20] J.C. Crittenden, N.J. Hutzler, D.G. Geyer, J.L. Oravitz, G. Friedman, Transport of organic compounds with saturated groundwater flow: Model development and parameter sensitivity, Water Resour. Res. 22 (1986) 271–284.
[21] D.W. Hand, J.C. Crittenden, D.R. Hokanson, J.L. Bulloch, Predicting the performance of fixed-bed granular activated carbon adsorbers, Water Sci. Technol. 35 (1997) 235–241.
[22] K.A. Mertz, F. Gobin, D.W. Hand, D.R. Hokanson, J.C. Crittenden, Manual: Adsorption Design Software for Windows (Ad-DesignS), Michigan Technological University, Houghton, Michigan, 1999.
[23] W.J. Weber, E.H. Smith, Simulation and design models for adsorption processes, Environ. Sci. Technol. 21 (11) (1987) 1040–1050.
[24] E.H. Smith, W.J. Weber, Modeling activated carbon adsorption of target organic-compounds from leachate-contaminated groundwaters, Environ. Sci. Technol. 22 (3) (1988) 313–321.
[25] M. Badruzzaman, P. Westerhoff, D.R.U. Knappe, Intraparticle diffusion and adsorption of arsenate onto granular ferric hydroxide (GFH), Water Res. 38 (18) (2004) 4002–4012.
[26] P. Westerhoff, D. Highfield, M. Badruzzaman, Y. Yoon, Rapid small-scale column tests for arsenate removal in iron oxide packed bed columns, J. Environ. Eng.-ASCE 131 (2) (2005) 262–271.
[27] R.F. Benenati, C.B. Brosilow, Void fraction distribution in bed of spheres, AIChE J. 8 (3) (1962) 351–361.
[28] C.F. Chu, K.M. Ng, Flow in packed tubes with a small tube to particle diameter ratio, AICHE J. 35 (1) (1989) 148–158.
[29] M.A.H. Franson, A.D. Eaton, L.S. Clesceri, A.E. Greenberg (Eds.), Standard Methods for the Examination of Water and Wastewater, 19th ed., American Public Health Association, Washington DC, USA, 1995.
[30] H.F. Lecoanet, M.R. Wiesner, Velocity effects on fullerene and oxide nanoparticle deposition in porous media, Environ. Sci. Technol. 38 (16) (2004) 4377–4382.
[31] S. Dukhin, C. Zhu, R.N. Dave, Q. Yu, Hydrodynamic fragmentation of nanoparticle aggregates at orthokinetic coagulation, Adv. Colloid Interface 114 (2005) 119–131.

[32] H. Jézéquel, K.H. Chu, Removal of arsenate from aqueous solution by adsorption onto titanium dioxide nanoparticles, J. Environ. Sci. Heal. A 41 (2006) 1519–1528.
[33] Q. Chen, G.H. Du, S. Zhang, L.M. Peng, The structure of trititanate nanotubes, Acta Crystallogr. B B58 (2002) 587–593.
[34] Q. Chen, W. Zhou, G.H. Du, L.M. Peng, Trititanate nanotubes made via a single alkali treatment, Adv. Mater. 14 (17) (2002) 1208–1211.
[35] A. Sperlich, A. Werner, A. Genz, G. Amy, E. Worch, M. Jekel, Breakthrough behavior of granular ferric hydroxide (GFH) fixed-bed adsorption filters: modeling and experimental approaches, Water Res. 39 (6) (2005) 1190–1198.
[36] P. Westerhoff, Arsenic Removal with Agglomerated Nanoparticle Media, AWWA Research Foundation, Denver, Colorado, USA, 2006.
[37] D.T. Hobbs, M.J. Barnes, R.L. Pulmano, K.M. Marshal, T.B. Edwards, M.G. Bronikowski, S.D. Fink, Strontium and actinide separations from high level nuclear waste solutions using monosodium titanate 1. Stimulant testing, Separ. Sci. Technol. 40 (2005) 3093–3111.
[38] F.F. Fondeur, D.T. Hobbs, M.J. Barnes, T.B. Peters, S.D. Fink, Kinetics and equilibrium sorption models. Fitting plutonium, strontium, uranium and neptunium loading on monosodium titanate (MST), Separ. Sci. Technol. 41 (2006) 2429–2445.
[39] S.P. Mishra, K.S. Vinod, D. Tiwari, Radiotracer technique in adsorption study 16. An efficient removal of cadmium by sodium titanate from aqueous solutions, Appl. Radiat. Isotopes 48 (4) (1997) 435–440.
[40] M.M. Abou-Mesalam, Retention behavior of nickel, copper, cadmium, and zinc ions from aqueous solutions on silico-titanate and silico-antimonate used as inorganic ion exchange materials, J. Radioanal. Nucl. Chem. 252 (3) (2002) 579–583.